Experimental Investigation of the Free Surface Effect on the Conical Taylor-Couette Flow System

F. Yahi[1,2], Y. Hamnoune[1], A. Bouabdallah[1], S. Lecheheb[1] and F. Mokhtari[1]

[1] *Thermodynamics and Energetic Systems Laboratory, Faculty of Physics. University of Sciences and Technology Houari Boumediene, B.P.32 El Alia 16111 Bab Ezzouar. Algiers, Algeria.*
[2] *Genie Physical of hydrocarbons Laboratory Faculty of hydrocarbons and chimestry, University M'Hamed Bougara–35000 Boumerdes-Algeria*

†*Corresponding Author Email: Yahi.fatma@gmail.com*

ABSTRACT

The aim of this work is to highlight the critical thresholds corresponding to the onset of different instabilities considered in the flow between two vertical coaxial cones with and without free surface. The inner cone is rotating and the outer one is maintained at rest. Both cones have the same apex angle $\Phi = 12°$ giving a constant annular gap $\delta = d/R_{1max}$. The height of the fluid column is H=155mm and It can be progressively decreased for each studied case of the flow system. Two kinds of configurations are studied, small and large gap. The working fluid is assumed as Newtonian and having constant properties like density and viscosity within the range of the required experimental conditions. By means of visualization technique of the flow we have been able to show the different transition modes occurring in the conical flow system according to the aspect ratio and then the induced action of the free surface which introduces a delay in the onset of different instability modes. The obtained results in term of features and stability of the flow are compared to those of Wimmer and Noui-Mehidi.

Keywords: Rotating cones; Taylor-Couette flow; Spiral wave; Free surface, Aspect ratio; Wavy mode.

NOMENCLATURE

d	annular radial gap	λ^*	Dimensionless wavelength number
DHM	Downward Helical Motion	Γ	aspect ratio
H	maximum length of the fluid column	Φ	apex angle
h	length of the fluid column	δ	radial gap
n	cell number	ν	kinematic viscosity
R_{1max}	largest radius of the inner cone	ρ	density
R_{1min}	lowest radius of the inner cone		
R_{2max}	largest radius of the outer cone	**Dimensionless numbers**	
R_{2min}	lowest radius of the outer cone		
TVF	Taylor Vortices Flow	$Fr = R_{1max}\Omega/\sqrt{gh\cos\phi}$	Froude number
UHM	Upward Helical Motion	$Re = R_{1max}\Omega d/\nu$	Reynolds number
WVF	Wavy Vortices Flow	$Ta = \sqrt{T} = Re\sqrt{\delta}$	Taylor number
V^*	dimensionless axial velocity	Tc	Critical Taylor number

1. INTRODUCTION

The flow between rotating coaxial cylinders has been the subject of numerous theoretical and experimental works. Taylor (1923) was the first author who predicted the onset of the first instability: axial stationary wave consists of two contra-rotating vortices. Thereafter, this kind of rotational motion has been generalized to various geometries such as flow between coaxial spheres and between coaxial cones. As well as in industrial processes, this flow system has a great importance, not only in the design of rotating machinery such as multiple concentric drives, turbine rotor, but also for the application in the chemical equipment such as compact rotating heat exchangers and mixers.

The flow between rotating cones has been studied

experimentally and numerically by several authors. Wimmer (1975 and 1988) has studied Taylor-Couette flow in different geometries: cylindrical, spherical, conical and between coaxial ellipsoids. he has investigated the combination between cone and cylinder. Noui Mehidi *et al.* (1993) have examined the laminar-turbulent transition in the case of small gap configuration and they have showed that the flow develops from the laminar regime towards helical motion through the formation of Taylor vortices by varying the rotation speed of the inner cone. In 1995, Wimmer investigated the appearance of Taylor vortices in different gap configurations, with the inner rotating and the outer at rest, and he found that the basic flow is three dimensional. Noui Mehidi and Wimmer (1999) studied the flow states occurring in the presence of free surface in the case of large gap configuration.

In this work, we consider the conical Taylor-Couette flow with small and large gap configurations. Our primary interests are to carry out a systematic experimental study, focusing on analysis of laminar-turbulent regime to highlight the transition process from order to disorder including the appearance of different instability modes until we observe the triggering of the chaos. In the Light of the work of Noui Mehidi and Wimmer (1999) as well as the work of Mahamdia (1990-2003 and 2008) devoted to the effect of free surface on Taylor-Couette flow. We are motivated to perform this study which will allow us to highlight the influence of the free surface on viscous fluid flow between two coaxial cones whose inner cone is rotating and the outer one is at rest. Two kinds of configurations have been investigated, large and small gap in order to highlight the effect of the free surface that has been studied only in the wide gap configuration ($\delta = 0.25$). The main purpose of our study is to derive a comparison between the present case (small gap) and the nominal case existed in the specialized literature (large gap). The effect of free surface on the onset of different instability modes, cells number, axial wavelenght and axial velocity is systematically examined. The obtained results are compared with those of Wimmer and Noui Mehidi in the case of large gap configuration.

2. EXPERIMENT DEVICES

The experimental device consists of two coaxial cones made of insulating and transparent material (Plexiglas) in order to allow a good visualization of flow regime. Both cones have the same apex angle $\Phi=12°$ giving a constant annular gap $\delta = d/R_{1max}$ where $d = (R_{2max}-R_{1max})$. The inner cone is rotating and the outer one is maintained at rest.

Two kinds of configuration have been investigated: a small annular gap configuration $d_1 = (4.85\pm 0.2)$ mm and large annular gap $d_2 = (9.68\pm 0.2)$ mm. Our system is characterized by an outer cone with largest radius $R_{2max} = (45\pm 0.2)$ mm and lowest radius $R_{2min} = (12\pm 0.2)$ mm. The length of the fluid column is fixed at $H = (155\pm 0.2)$ mm. The largest radius of the inner cone R_{1max} varies between (40.15 ± 0.2) mm and (35.31 ± 0.2) mm, while the lowest radius R_{1min} ranges from (7.15 ± 0.2) mm and (2.32 ± 0.2) mm.

The inner cone is driven by a DC motor connected to the rotating axis by a flexible in order to avoid the adverse effects of vibration, (Fig. 1).
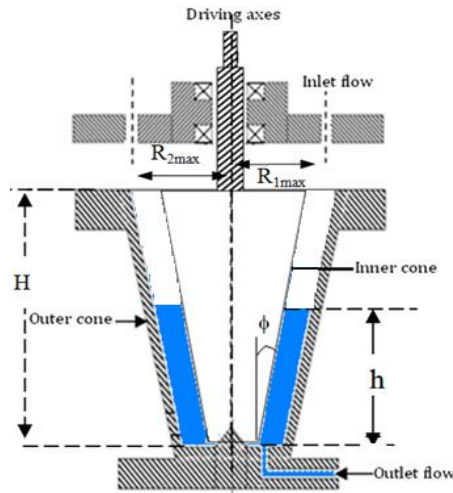

Fig. 1. Conical Taylor-Couette flow system.

The used display product is a solution of 20% of Vaseline oil CHALLALA, favoring a better suspension of the particles in the fluid visualization, which is added to 80% of a petroleum product SIMILI to reduce the viscosity of the oil in a concentration of 2g/l of aluminum flakes. Such that the mixture constitutes a Newtonian fluid characterized by kinematic viscosity $\nu=4.8\ 10^{-6}\ m^2/s$ and a density $\rho = 777.23 kg/m^3$ with an accuracy of 1%.

In order to characterize the onset of hydrodynamic instabilities, it is necessary to introduce dimensionless numbers involving viscous forces that play a stabilizing role and centrifugal forces which have a destabilizing effect. The manifestation of a given waveform or instability was identified using the control parameters of flow namely, Reynolds number Re, Taylor number Ta and Froude number Fr defined in table 1:

Table 1 Control parameters

| Geometric		Dynamic
$\delta = \dfrac{d}{R_{1max}}$	$\delta_1=0.12$ (small gap)	Reynolds number $Re = \dfrac{R_{1max}\Omega d}{\nu}$
	$\delta=0.27$ (large gap)	Taylor number $Ta = Re\delta^{1/2}$
$\Gamma=h/d$	$9.6< \Gamma_1<32$ $3.1< \Gamma_2<16$	Froude number Fr $= \dfrac{R_{1max}\Omega}{(ghcos\phi)^{1/2}}$

During the experiments, we have used a digital camera Sony Cyber-Shot. The DSC-T20, with eight mega pixels which has a sensor coupled to a 3X optical zoom and a 2.5 inch LCD screen with an optical image stabilizer. The T20 also offers high

definition video output and a storage capacity of 128 MB up to 8GB. The camera gives picture MPEG VX Fine 640 x 480 with 30 images/sec, MPEG VX Standard 640 x 480 with 16 images/sec and MPEG 320 x 240 with 8 images/sec.

Three visualization techniques have been used:

2.1 Reflection of Natural Light

This method is based on the light beam reflecting from seeding particles. The light is supplied by an external source located in front of the experimental device, in order to highlight the nature and the properties of the flow structure. The mechanism of this technique is about properties of reflected light depending on the orientation of the velocity vector. If it is axial, the particles will reflect light completely and the current case gives us the maximum velocity of the cell. On the contrary, if the velocity has a significant radial component, the particles will be oriented parallel to the light rays and they will let the light pass without reflection. In that case the velocity is minimal (Fig. 2).

Helicoidal vortices
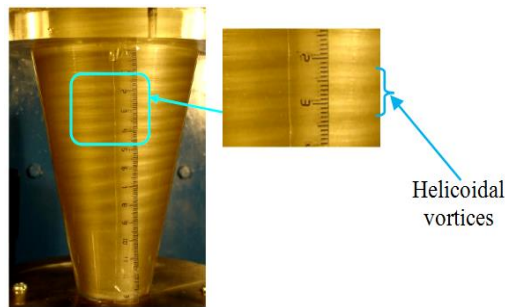
Fig. 2. Natural light reflection $\delta_1 = 0.12$, $\Gamma = 32$ Ta = 64.9.

2.2 Transmission of Natural Light:

This method of visualization is based on the optical transmission of the light source which is placed behind the experimental device. The light rays pass through the flow and provide in-depth structure of the flow which can allow us to observe clearly the inclination of the cells with respect to horizontal plane (Fig. 3).


Helicoidal vortices
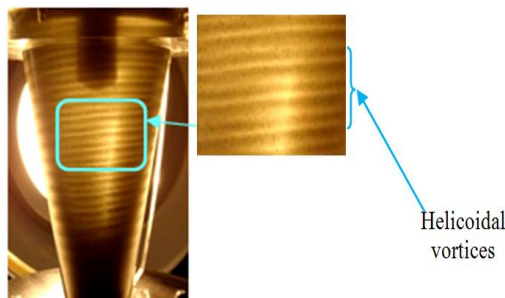
**Fig. 3. Natural light transmission $\delta_1 = 0.12$, $\Gamma = 32$ Ta = 72.**

2.3 Laser Transmission

In order to examine the local structure of the movement, we have used coherent light (laser He, 1mW and with wavelength $\lambda = 623.8$nm). It shows us the detailed configuration of Taylor vortices. The projection of the light plane of the laser is effected in a vertical plane by means of a cylindrical lens of a diameter D. the required need of the experiment is to see all the local structure of the flow or to isolate a cell. For that it is imperative to respect the following adequate distances (D = 12mm, $l_1 = 26$mm, $l_2 = 37$mm) for converging the beam and obtaining a rigorous stigma of the image corresponding to the considered object (Fig. 4:- a and -b).
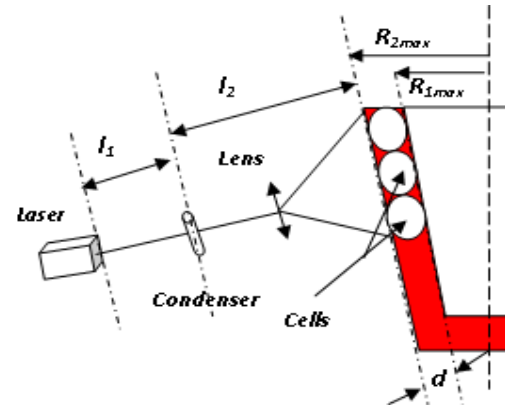
a)
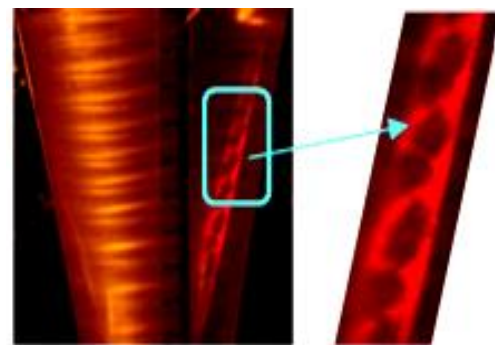
b)

Fig. 4. a) - Laser transmission visualization layout b) - Laser transmission visualization $\delta_1 = 0.12$, $\Gamma = 25.8$ Ta = 88.5.

3. RESULTS AND DISCUSSIONS

For both configurations, small $\delta_1 = 0.12$ and large annular gap $\delta_2 = 0.27$ and for a given aspect ratio Γ in the interval $9.6 < \Gamma_1 < 32$ and $3.1 < \Gamma_2 < 16$, we investigate the basic flow and the laminar-turbulent transition regime.

3.1 Basic Flow

The basic flow is laminar three-dimensional for Ta < Tc_1 in the whole range of aspect ratio Γ. It is a result of the imbalance between the viscous and centrifugal forces that exist in the absence of any disturbance. The three-dimensional nature of the flow is mainly due to the linear variation of the centrifugal forces caused by the linear variation of the radius versus the conical axial position "z". The flow is a homogeneous movement throughout the fluid column, characterized by a perfect symmetry in the axial and azimuthal directions.

3.2 Transition Regimes

3.2.1 Completely Filled System

For a completely filled system, the fluid is limited by the end plates where the non-slip condition is applied. It causes a deceleration of the fluid. For a constant radial gap and by increasing the angular velocity of the inner cone, the centrifugal forces will progressively dominate the viscous forces. The disturbances of the basic flow then generate regular closed vortex cells. The first cell of Taylor appears in the vicinity of the upper edge where the centrifugal forces are greater. This toroidal cell is stationary and its size is of the order of the annular gap and forms a pair of cells with the rest of the flow. The Taylor number value corresponding to the appearance of the Taylor vortex (TV) is $Ta = Tc_1$. By increasing the inner cone velocity gradually we observe the appearance of a second cell that propagates along the downward helical motion which is characterized by the Taylor number $Ta = Tc^{DHM}$. The principal reason of this downward movement of the vortex is the rotation of the cell around itself and the mass transport is compensated in such a helical vortex tube. Near $Ta = Tc_1$ we note the formation of two different flow zones: one evolving is in a supercritical flow regime (unstable laminar flow) and the other one is governed by a subcritical flow regime (laminar stable) (Fig. 5). The azimuthal wave or "the Wavy Mode" appears in the upper part of the annulus with a very low amplitude corresponding to the critical Taylor number $Ta = Tc_2$. Then the other part of the cells preserves the same properties as those described above. The existence of this second instability produces a doubly periodic flow which propagates in the axial and azimuthal directions. For $Ta = Tc^{UHM}$ corresponding to the appearance of the upward helical motion of cells, we note the superposition of three flow instabilities, namely, downward helical motion (DHM), upward helical motion (UHM) and wavy mode (WM) (Figs. 5-b).
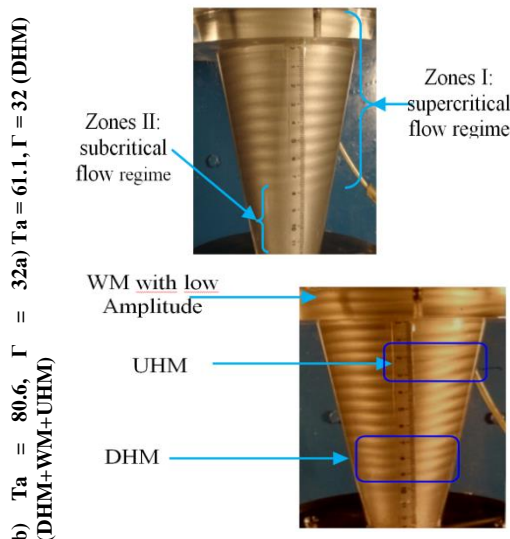
obtained results are in a good agreement with those of Wimmer in the case of a small annular gap. The Taylor number value corresponding to the onset of the Taylor vortices in the case $\delta_1 = 0.12$ is close to that obtained by Wimmer (1995) for a radial gap $\delta = 0.11$. It is also very close to that obtained in the cylindrical geometry near to 2.4% for a small gap configuration. Whereas, the discrepancy was 5.6% for the downward helical motion. This value coincides with that obtained in spherical geometry Ts = 57.62 evaluated at 3.2% in the case $\delta = 0.14$. In addition, the discrepancy corresponding to the appearance of the azimuthal wave is 7.7% compared with the work of Wimmer.

Table 2 Comparison of critical Taylor number values for different gap configurations (completely filled flow system)

Critical Taylor Number	Tc_1	Tc^{DHM}	Tc_2	Tc^{UHM}
Flow Regimes	TVF	DHM	WVF	UHM
Wimmer $\delta = 0.11$	41.6	50	74.9	
Present work $\delta_1 = 0.12$	42.3 1.7%	47.2 5.6%	68.8 7.65%	72
Wimmer $\delta = 0.25$	46.7	57	68	-
Present work $\delta_2 = 0.27$	65.8 41.5%	85.1 25%	145.6	189.3

In the case of a large gap configuration $\delta_2 = 0.27$, it is found that the relative discrepancy in the Taylor number value corresponding to the onset of the (TV) becomes very large 41.5. While the one corresponding to the establishment of the downward helical motion is about 25% because when the annular spaces becomes larger, the instabilities installation becomes slower and introduces an onset delay.

Some flow states for the small gap configuration corresponding to $\delta_1 = 0.12$ are shown in (Fig. 6).

3.2.2 Partially Filled System

In the presence of free surface a strong deceleration cannot take place. Thus the angular velocity in the vicinity of free surface is higher than the one near the stationary end plate. The higher velocity leads to increase centrifugal forces resulting in the appearance of instabilities.

For the partially filled flow system $\Gamma < 32$, the existence of a vortex ring induced by the free surface is observed before the onset of the Taylor vortex. This so-called free surface cell undergoes torsion during the appearance of the first steady cell which is settled in the vicinity of the free surface (Fig. 7).
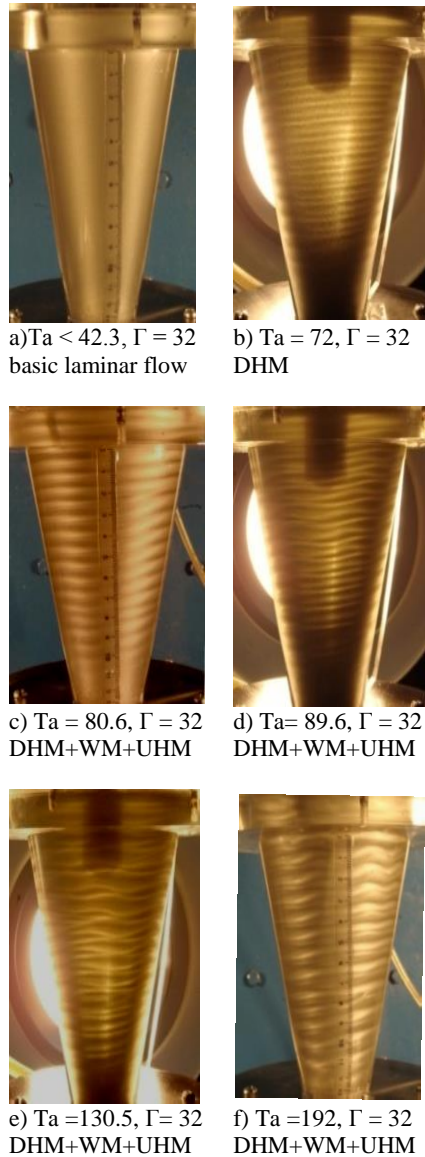

a) $\Gamma = 32$ $Ta = 61.1, \Gamma = 32$ (DHM)

Zones I: supercritical flow regime

Zones II: subcritical flow regime

b) $Ta = 80.6$, $\Gamma = 32$ (DHM+WM+UHM)

WM with low Amplitude

UHM

DHM

Fig. 5. a) -**Visualization of sub and supercritical regime , b)- superposition of three flow instabilities.**

By the observation of table2, we can see that the

a)Ta < 42.3, Γ = 32
basic laminar flow

b) Ta = 72, Γ = 32
DHM

c) Ta = 80.6, Γ = 32
DHM+WM+UHM

d) Ta= 89.6, Γ = 32
DHM+WM+UHM

e) Ta =130.5, Γ = 32
DHM+WM+UHM

f) Ta =192, Γ = 32
DHM+WM+UHM

Fig. 6. Flow visualization states: a), c) and f) Natural light reflection. b), d) and e) Natural light transmission δ₁ = 0.12.
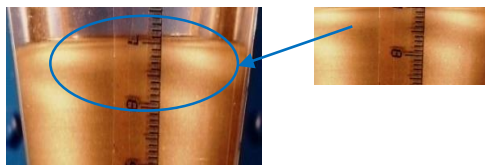

Fig. 7. Warping phenomenon visualization.

The analysis of this vortex has allowed us to determine the evolution of its size "e" in function of filling ratio, as well as its angle θ with respect to the horizontal axis. The size of this vortex is higher for low aspect ratio $9.6 \leq \Gamma \leq 17.5$ (e = 9mm). Then it tends to decrease to a value of 0 for Γ = 32 according to a polynomial law. However, the angle θ decreases as an exponential function (Fig. 8).
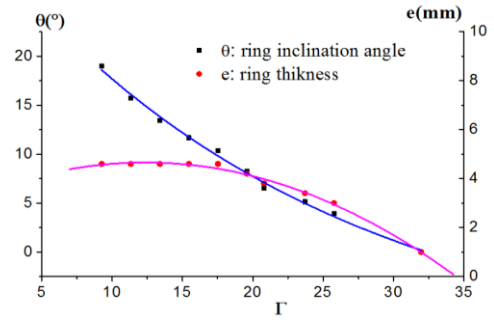

Fig. 8. Evolution of the thickness and the inclination angle of the ring in the vicinity of the free surface.
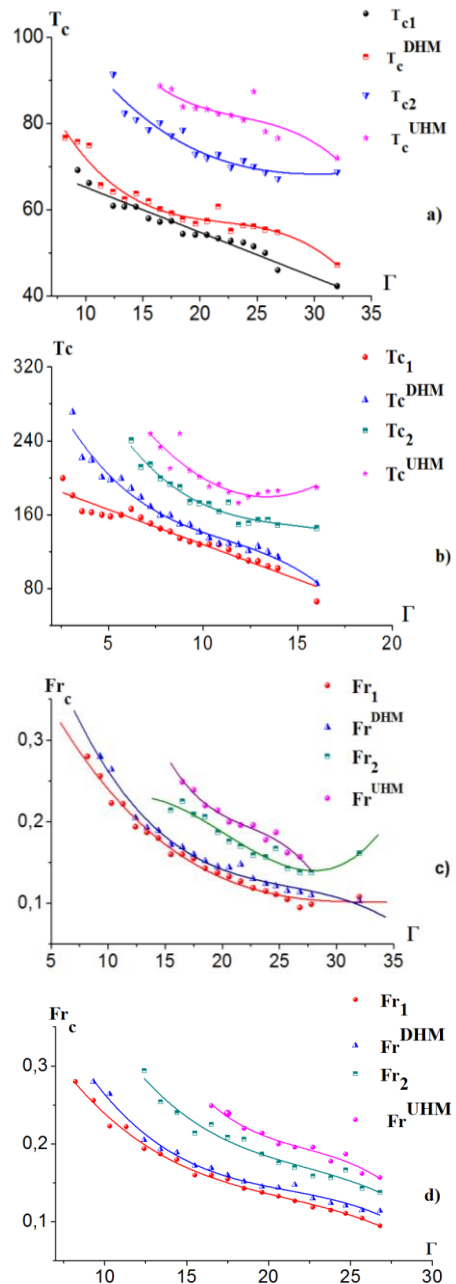

Fig. 9. Evolution of the critical Taylor number (a, b) and the critical Froude number (c, d) depending on the filling rate Γ for both configurations.
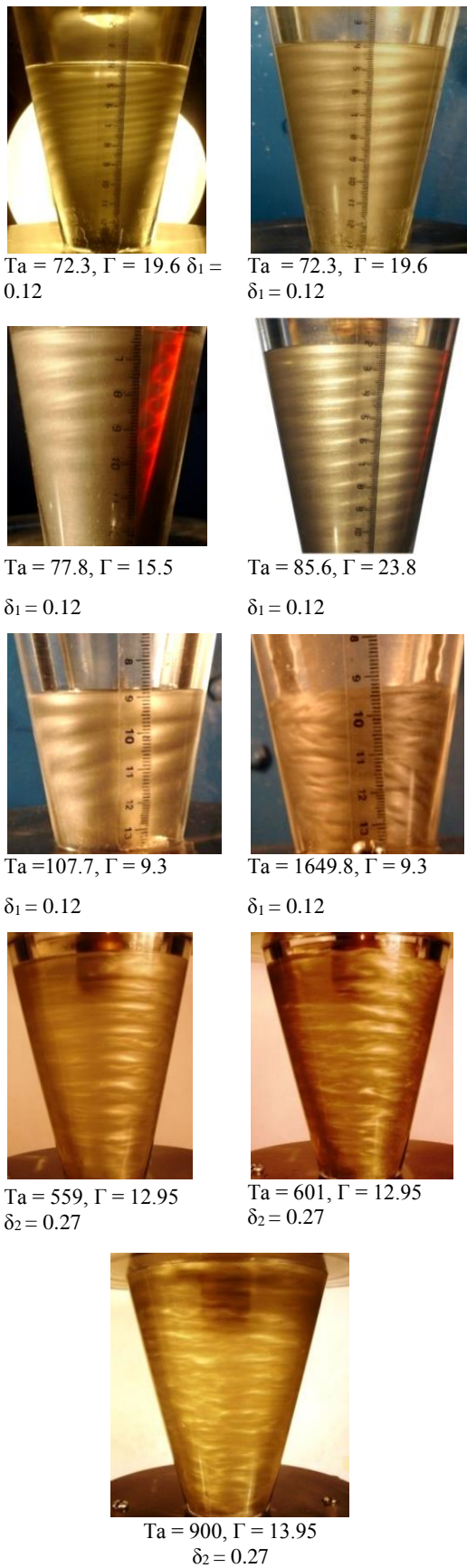
Ta = 72.3, Γ = 19.6 δ₁ = 0.12

Ta = 72.3, Γ = 19.6 δ₁ = 0.12

Ta = 77.8, Γ = 15.5 δ₁ = 0.12

Ta = 85.6, Γ = 23.8 δ₁ = 0.12

Ta =107.7, Γ = 9.3 δ₁ = 0.12

Ta = 1649.8, Γ = 9.3 δ₁ = 0.12

Ta = 559, Γ = 12.95 δ₂ = 0.27

Ta = 601, Γ = 12.95 δ₂ = 0.27

Ta = 900, Γ = 13.95 δ₂ = 0.27

Fig. 10. Visualization of flow in presence of a free surface for various Taylor number in both configurations.

For small gap configuration $\delta_1 = 0.12$ and different filling ratio values $9.6 \le \Gamma < 32$, the first cell is inclined in the opposite direction of the free surface vortex. The first instability (TVF) is delayed for 11% to 66% compared to the completely filled flow system. Whereas for relatively large configuration $\delta_2 = 0.27$ this delay is more important and It is between 55% and 200%. The Taylor number corresponding to the first instability changes according to a linear law with negative slope of (-1.1). In addition, the Froude number evolves according to a polynomial law with aspect ratio Γ in the range $9.6 \le \Gamma < 32$ in the case of the small gap configuration $\delta_1 = 0.12$.

The Azimuthal wave is delayed 16% to 60%, up to a critical height $\Gamma_c = 15.5$. At this threshold $\Gamma = \Gamma_c$, the wavy mode disappears (Fig. 9 -a). This delay is produced by the free surface and it is mainly due to the meridional component velocity of the flow.

3.3 Evolution of Cells Number and Wavelength for Different Flow Regimes

The analysis of the results in the case of small gap configuration shows clearly the evolution of the cells number according to the flow regime. For $\Gamma = 32$, the vortices number starts with one cell in the vicinity of first instability (TVF) corresponding to Ta=42.3 and then it continues in increasing to reach the maximum value. Therefore, It stabilizes at that value until Ta=192. After that, subsequently, it stabilizes in another range of Taylor number. By increasing Taylor number more and more we observe the decreasing of cells number "n" (Fig. 11: -a, -b).
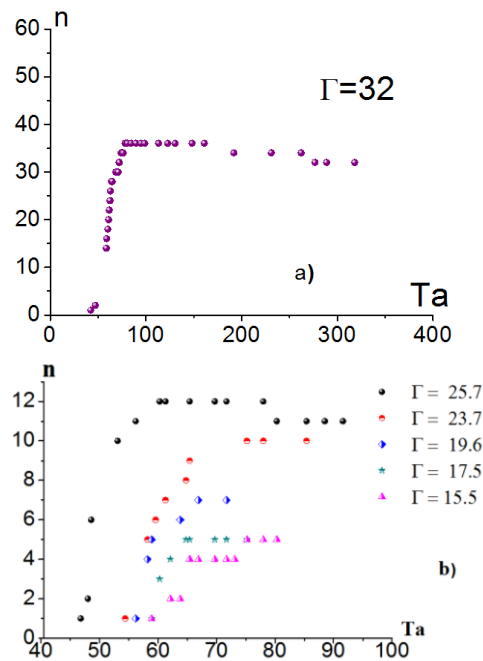

Fig. 11. Variation of the cell number n versus Taylor number Ta: (a) - Completely filled system Γ = 32, (b) –Partially filled system Γ < 32 & δ1 = 0.12.

The evolution of the dimensionless axial wavelength λ^* depending on the Taylor number Ta, for a

completely filled flow system, decreases exponentially. It passes through a maximum value 0.9737. Then it decreases and tends to stabilize towards a value of 0.628 corresponding to 2/3 of the maximum value and remains constant in the range $68.8 < Ta < 350$. This result was established by Bouabdallah in the cylindrical Taylor-Couette flow system in the case of a small gap configuration $\delta = 0.10$. By decreasing the filling ratio progressively, we observe that the behavior law changes as shown in (Fig. 12: a-b & c). It was found that for $\Gamma = 32$, $\Gamma = 25.7$, $\Gamma = 23.8$ and $\Gamma = 9.3$ the axial wavelength follows the same law behavior. However, in the case of the $\Gamma = 17.5$ and $\Gamma = 15.5$ the wavelength increases exponentially.
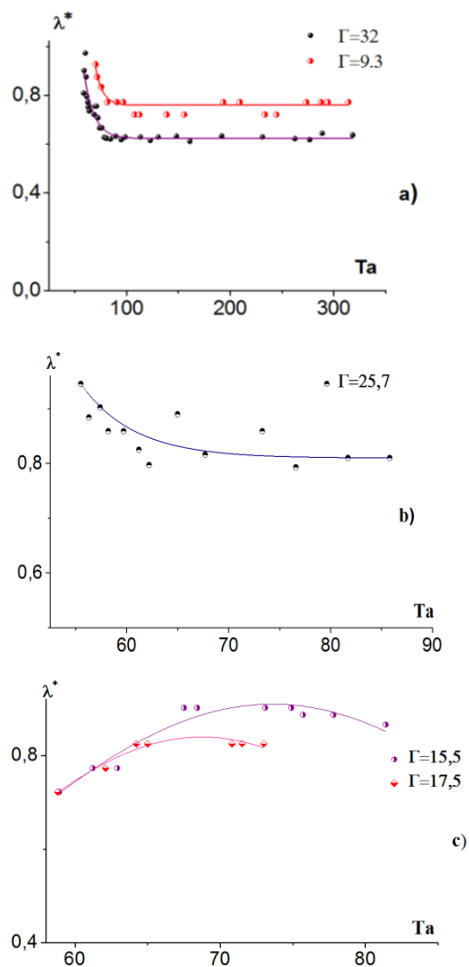

Fig. 12. Evolution of axial wavelength λ* versus Taylor number Ta: a) - Completely filled system Γ = 32 and Γ = 9.3, b) & c) – Partially filled system 9.3 < Γ < 32 & δ₁ = 0.12.

3.4. Evolution of the Axial Velocity Vz* in Function of the Taylor Number Ta

Regarding to the evolution of the axial velocity $Vz^* = Vz/V_1$ in function of Taylor number in the completely filled system, we note that Vz^* begins at the maximum value $Vz^* = 0.053$. Therefore, it decreases until it becomes almost constant. These results are substantially similar to those obtained by Wimmer.

For a filling ratio $\Gamma = 25.7$, we find that the dimensionless axial velocity corresponds to the same behavior as $\Gamma = 32$. For $\Gamma = 9.3$ this behavior may change considerably in the range: $75.4 < Ta < 209$ it evolves according to an exponential law. Beyond $Ta = 209$ the dimensionless axial velocity Vz^* varies according to a linear law (Fig. 13 - c).
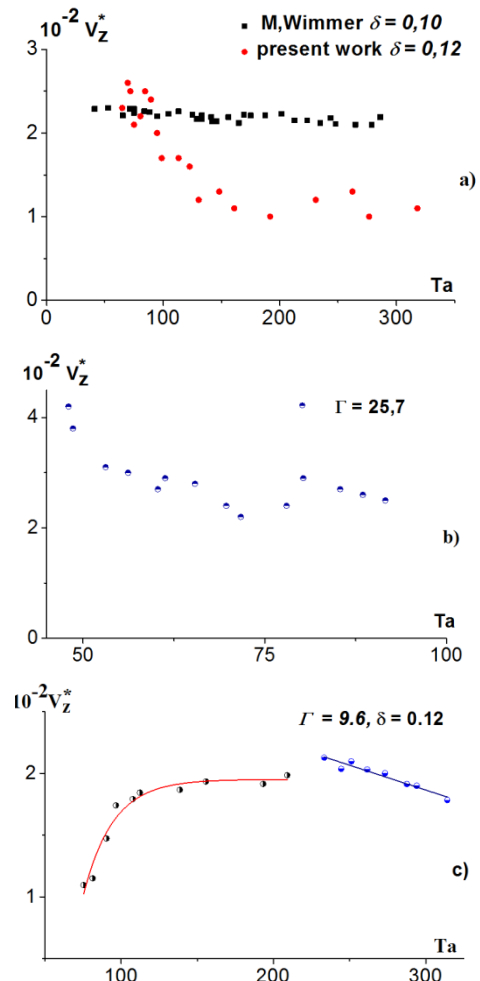

Fig. 13. Evolution of the axial velocity versus Taylor number; (a) Γ = 32 completely filled flow system (b, c) Γ = 25.7 and Γ = 9.3 partially filled flow system & δ1 = 0.12.

5. CONCLUSION

The flow behavior of the fluid between two coaxial conical cylinders with the inner cone rotating and the outer one stationary was studied experimentally. Special attention was paid to the effect of free surface on the conical Taylor-Couette flow.

The present experiments indicate that chaotic regime occurs after a small number of transitions. We can distinguish four instability modes: Taylor vortices mode, downward helical motion, wavy mode and upward helical motion in the small and large configurations. In the case of completely filled flow system there is a direct transition to chaos. While in the case of partially filled flow system there are some modifications preceding turbulence.

For $\Gamma < 32$, a vortex ring induced by the free surface is observed before the onset of the Taylor vortex. This so-called free surface cell undergoes torsion during the appearance of the first steady cell which is settled in the vicinity of the free surface.

The axial limitation of the flow introduces a considerable delay in the appearance of the first instability (Taylor vortices), the onset of spiral wave and azimuthal wave as well. In particular, we observe the disappearance of the azimuthal wave for a critical value of aspect ratio $\Gamma = \Gamma c_1 = 15.5$ ($\delta_1 = 0.12$) and $\Gamma = \Gamma c_2 = 6.7$ ($\delta_2 = 0.27$).

The major interest in these experiments in both cases of flow system configurations is the properties of the free surface, such as the interaction on the mode formations. Its characteristics: axial wavelength, axial velocity and globally a stabilizing effect of the whole movement in the conical Taylor-Couette flow system.

The research reported here will be continued with experiments by spectral analysis on selective Γ with increased the Taylor number Ta aiming to determining the evolution of different instability modes in laminar-turbulent transition.

REFERENCES

Adnane, E., A. Lalaoua and A. Bouabdallah (2016). An experimental study of the laminar-turbulent transition in a tilted Taylor-Couette system subject to free surface effect. *Journal of Applied Fluid Mechanics 9 (4).*

Bouabdallah, A. (1980). *Instabilités et Turbulence dans l'écoulement de Taylor-Couette*. Ph. D. thesis, INP Lorraine.

Hofmann, N. P. and F. H. Busse (1999). Instabilities of shear flows between two coaxial differentially rotating cones. *Phy. F 11*

Kádár, R. and C. Balan (2012). Transient dynamics of the wavy regime in Taylor–Couette geometry. *Eur. J. M. B/Fluids 31, 158-167.*

Lalaoua A. and A. Bouabdallah, (2016). On the onset of Taylor vortices in finite-length cavity subject to a radial oscillation motion. *Journal of Applied Fluid Mechanics 9 (4).*

Lalaoua, A. and A. Bouabdallah (2016). On the onset of Taylor vortices in finite-length cavity subject to a radial oscillation motion. *Journal of Applied Fluid Mechanics 9 (4).*

LI, Q. S., P. Wen, L. X. XU (2010). Transition to taylor vortex flow between rotating conical cylinders. *J. hydro. 22, 241-245.*

Mahamdia, A., A. Dhaoui and A. Bouabdallah (2008). Aspect ratio influence on the stability of Taylor-Couette flow. *Journal of Physics Conference Series (137).*

Mahamdia A., and A. Bouabdallah (2003). Effets de la surface libre et du rapport d'aspect sur la transition de l'écoulement de Taylor- Couette. *CRAS -Paris Mécanique 331(3), 245-252.*

Mahamdia, A., and A. Bouabdallah (1990). Effets simultanés des limitations axiale et radiale sur l'écoulement de Taylor-Couette. *Modelling, Measurement and Control, B, AMSE Press 30(1), 5-12.*

Nakabayashi, K., Z. Zheng and Y. Tsuchida (2003). Characteristics of disturbances in the laminar–turbulent transition of spherical Couette flow. 1. Spiral Taylor–Goertler vortices and traveling waves for narrow gaps. *Phys. Fluids 14, 39-63.*

Noui-Mehidi, M. N. and A. Bouabdallah (1993). A laminar-turbulent transition in the flow between rotating coaxial cones. In *Proc. 3rd Int. Workshop on electrodiffusion diagnostics of flow, CNRS 139-147.*

Noui-Mehidi, M. N., N. Ohmura and K. Kataoka (2001). An Experimental Investigation of Flow Mode Selection in a Conical Taylor – Couette System. *Int. J. F. Dyna. 5, Article 1.*

Noui-Mehidi, M. N., N. Ohmura and K. Kataoka. (2001, *September*). Flow modes selection and transition in conical cylinders system. *12th I. C.T.W, 6-8.*

Noui-Mehidi, M .N. and *et al*. (2005). Dynamics of the helical flow between rotating conical cylinders. *J. F. S. 20, 331-334*

Noui-Mehidi, M. N. and *et al*. (2009). Effect of wall alignment in a very short rotating annulus. Commun. *Nonlinear Sci. Numer. Simulat. 14(2), 613-621,*

Noui-Mehidi, M. N. and M. Wimmer (1999). Free surface effects on the flow between conical cylinders. *Acta Mechanica 135, 13-25*

Noui-Mehidi, M. N., A. Salem, P. Legentilhomme and J. Legrand (1999). Apex angle effects on the swirling flow between cones induced by means of a tangential inlet. *Int. J. of Heat and Fluid Flow 20, 405-413.*

Noui-Mehidi, M. N. and *et al*. (2004). Gap Effect on Taylor Vortex Size Between Rotating Conical Cylinders. *15th Australasian Fluid Mechanics Conference*, Sydney, Australia

Noui-Mehidi, M. N., N. Ohmura and K. Kataoka (2002). Mechanism of mode selection for Taylor vortex flow between coaxial conical rotating cylinders. *Journal of Fluids and Structures 16, 247–262.*

Ohmura, N., M. N. Noui-Mehidi and *et al*. (2004). Mixing characteristics in a conical Taylor-Couette Flow System at Low Reynolds numbers. *J. Che. Eng. of Japan 37, 546-550*

Rapley, S. and *et al*. (2008). Computational investigation of torque on coaxial rotating cones. *J. Fluids Eng., 130(6)*

Sha, W. and K. Nakabayashi (2001). On the structure and formation of spiral Taylor-Gortler vortices in spherical Couette flow *J. F. M. 295, 43-60.*

Sobolik, V., T. Jirout, J. Havlica and M. Kristiawan

(2011). Wall Shear Rates in Taylor Vortex Flow. *Journal of Applied Fluid Mechanics 2 (4), 25-31*

Taylor, G. I. (1923). *Stability of a viscous liquid contained between two rotating cylinders*. Phil. Trans. R. Soc. London Ser. A 223, 289-343.

Wimmer, M. and J. Zierep (2000). Transition from Taylor vortices to cross-flow instabilities. *Acta Mechanica 140, 17-30*.

Wimmer, M. (1988). Viscous flows and instabilities near rotating bodies. *Prog. Aerospace Sci 25, 43-103*

Wimmer, M. (1995). An experimental investigation of Taylor vortex flow between conical cylinders. *J. F. M. 292, 205-227*.

Wimmer, M. (2000). Taylor vortices at different geometries. In: Egbers, C.and Pfister, G. (Eds.), *Physics of Rotating Fluids*. Springer, Berlin 195–212

Xiaofei, X., P. Wen and L. Xu (2010). Dapeng Cao, Occurrence of Taylor vortices in the flow between two rotating conical cylinders. *Com. Nonlinear Sci. Num. Sim. 15, 1228–1239*.